COMPARISON OF ACTIVE MAGNETIC BEARINGS WITH AND WITHOUT PERMANENT MAGNET BIAS

Christian Ehmann, Tilo Sielaff, Rainer Nordmann
Darmstadt University of Technology
Department Mechatronics and Machine Acoustics, Darmstadt, Germany
ehmann@mum.tu-darmstadt.de

ABSTRACT

A review of publications dealing with the design of active magnetic bearings reveals that some tend to a design with permanent magnets to create the bias flux, and others prefer a purely electric bias and control flux generation. The main scope of the paper is to compare both design principles, exemplarily for radial bearings. Interesting criterions are the negative stiffness, the coupling between the two radial force directions, the force/volume ratio and the number and complexity of necessary parts.

INTRODUCTION

Active magnetic bearings (AMB) are well-known components for the suspension of mechanical objects. For mechanical systems applicable for industry mainly such types using reluctance force are used, and in most situations two opposing electromagnetic poles allow control forces in two directions and take account of linearizing effects. This is beneficial for the position control which is indispensable since AMBs are unstable.

Even if only considering this class of AMBs there still are many different design principles, e. g. homopolar and heteropolar pole arrangements, bearings with and without bias flux, bearings using permanent magnets for bias flux, and there coplanar and non-coplanar arrangements of the bias and the control flux (Molenaar *et al.*, 1997), etc.

In this paper bearings with and without permanent magnets creating bias flux in non-coplanar arrangement shall be compared, referred to as I_0-type (the bias flux originates from a bias current) and PM_0-type (the bias flux originates from permanent magnets). Usually permanent magnets are used to save energy (zero current control) and reduce the number of power amplifiers or to minimize the size of the bearing (Lee *et al.*, 2000), especially when combining radial and axial bearing (McMullen *et al.*, 2000). Beyond these properties the permanent magnet should influence further parameters, especially the negative stiffness and the inductivity, which both are most important for the achievable control quality.

To investigate and compare those effects, first the basic principles are derived for a simple U-magnet. Next a homopolar and a heteropolar bearing of the PM_0-type are described, and an eight-pole I_0-type which is used for comparison. Beside analytical and finite element calculations measurements of the homopolar PM_0-type are presented.

SIMPLIFIED CONSIDERATIONS

In this section the basic effects derived from first principles are used to achieve a first comparison of both types. Geometry and important symbols are depicted in Figure 1.

MAGNETIC PRESSURE

The magnetic pressure helps to estimate the required size of the AMB for a desired load capacity. For strong gradients of the relative permeability, which

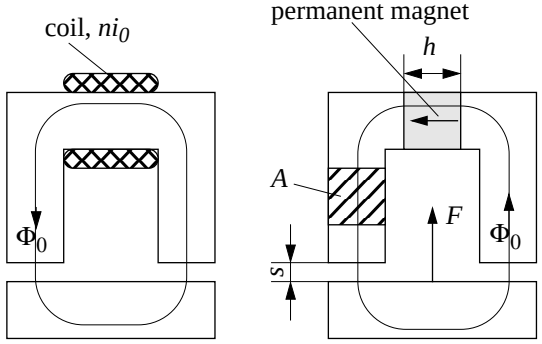

FIGURE 1: Geometry and symbols of the simplified magnetic circuits

occurs at the surface between iron and air ($\mu_{fe} \gg \mu_0$), the following equation holds (all subsequent equations for the electromagnetic actuator are taken from Schweitzer *et al.*, 1993, chap. 3)

$$p = \frac{F}{2A} = \frac{B^2}{2\mu_0}. \quad (1)$$

A typical flux density of 1 Tesla results in a magnetic pressure of 40 N/cm^2. The flux density $B = \Phi / A$ is a function of the current *ni* and the airgap *s*. We rather use the magnetic pressure *p* instead of the force *F* in order to better compare the different results later on.

NEGATIVE STIFFNESS

The negative stiffness $k_s = \partial F / \partial s|_{i = i0}$ is an inherent property of reluctance force actuators. This is a major drawback because much effort of the position controller is necessary to overcome the negative stiffness, limiting the achievable control quality. The correlation of the electromagnetic pressure and the airgap *s* is derived assuming that only the magnetomotive force for the permanent flux density B_0 is existing and that the magnetic resistance of the iron path and flux leakage is neglected. For the I_0-type

$$p_{I0} \approx \frac{\mu_0}{2} \cdot \left(\frac{ni}{2s}\right)^2 \quad (2)$$

holds. Meins (1997) gives a rough analytical solution for the PM_0-type,

$$p_{PM0} \approx \frac{B_r^2}{2\mu_0} \Big/ \left(1 + \frac{2s \cdot \mu_p}{h \cdot \mu_0}\right)^2, \quad (3)$$

where B_r is the remanence induction ($s = 0$) and μ_p the permeability of the permanent magnet, which normally is close to μ_0. Figure 2 shows the analytical solutions as well as 2D and 3D finite element (FE) calculations achieved with the program package FLUX (Cedrat, 2003). For the calculations the following parameters have been used: A = 15x15 mm, h = 20 mm, permanent magnet: NdFeB, remanence induction B_r = 1.1 Tesla. The current for the I_0-type has been chosen such that for s = 0.4 mm the flux density equals the 2D-FE solution. For the 2D and 3D FE calculations the same grid size has been used.

Following conclusions can be drawn: First, the gradient $\partial p / \partial s$ representing the negative stiffness is much larger for the I_0-type. Second, the comparison of the three solutions with the permanent magnet reveals that flux leakage has a major influence on the achievable flux density in the airgap. Since the 3D solution is very small, further calculations have been performed, where

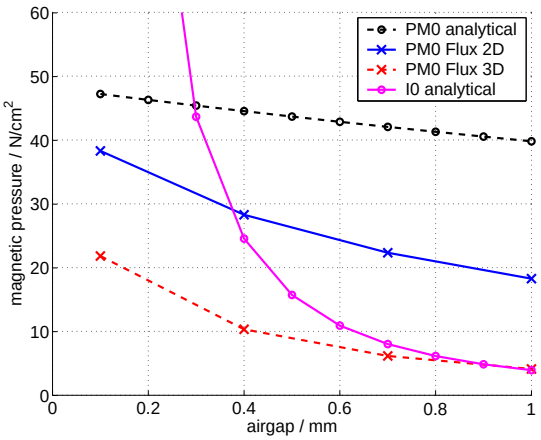

FIGURE 2: Magnetic pressure as function of the airgap

the depth of the U-magnet was much larger than all other dimensions. We expected that now the 3D solution would converge to the 2D solution at least in the centre of the magnet due to negligible flux leakage in the out of paper plane, but still the flux density was about 25 % below the 2D solution. Therefore the FE results of systems including permanent magnets might be inaccurate.

INDUCTIVITY

The inductivity of a bearing is important for dimensioning the power amplifiers. Generally speaking a low inductivity leads to a better dynamic behavior of the actuator. A common worst case estimation for the inductivity is

$$L = n^2 \mu_0 A \cdot \frac{1}{2s}. \quad (4)$$

The number of windings *n* again depends on the required maximum flux density in the bearing and on the maximum current of the power amplifiers. For better comparison we assume that the maximum current i_{max} shall be the same for all configurations, hence the maximum flux density

$$B_{max} = \mu_0 \frac{n \cdot i_{max}}{2s} \quad (5)$$

only depends on the number of windings for a given airgap *s*. Eliminating *n* by introducing (5) in (4) results in

$$L = \frac{2A}{i_{max}^2 \mu_0} \cdot B_{max}^2 \cdot s. \quad (6)$$

The inductivity and other properties of the magnetic bearings only can be described in context of the mechanical design, which will be introduced next.

AMB WITH PERMANENT MAGNETS

From the previous section it is obvious that the PM_0-type bearings should have a lower negative stiffness, which helps to improve the control behavior of such bearings. In this chapter two bearing arrangements will be described, which present extreme design principles for the non-coplanar arrangement.

HOMOPOLAR DESIGN

The first design illustrated in Figure 3 has a permanent magnetic ring on the rotor and thus allows a very compact design with only few parts. From the bias flux' Φ_0 point of view this is a homopolar arrangement. The depicted coils (the coils for the *x*-direction are not shown) are connected in series and have the same winding direction to create the control flux Φ_c. Φ_0 and Φ_c can be superimposed in the airgap. Hence, in the right sketch of Figure 3 both flux components are in the same direction in the upper airgaps and oppose each other in the lower airgaps, generating a reluctance force on the rotor in positive *y*-direction.

In the lower part of Figure 3 the geometry and results for the 2D-FE calculation are shown. Here the rotor was in the centre position and the control current was set to zero. Later, the results calculated with this 2D model will be compared with the 3D model depicted in Figure 4.

Here a major drawback concerning the negative stiffness can be recognized, which exists for all homopolar bias magnets, no matter if they are located in the rotor or in the stator (e. g. Mohr *et al.*, 2003): Due to the eccentric rotor position the magnetic resistance is

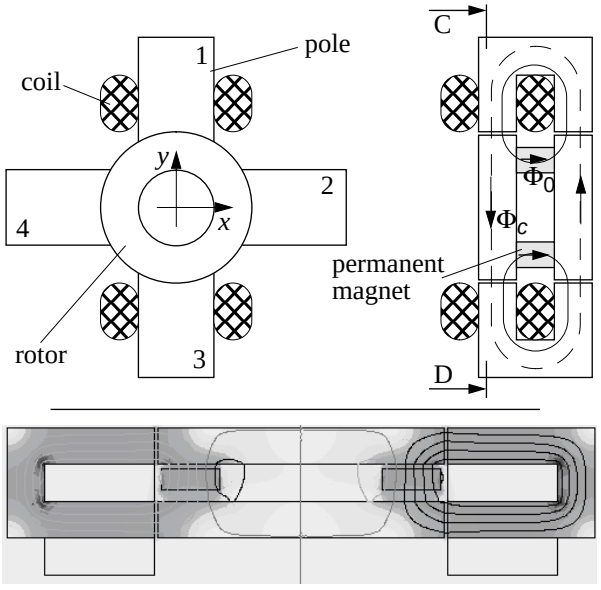

FIGURE 3: Homopolar design and calculated equiflux lines. The bias flux density in the airgap is 0.7 T

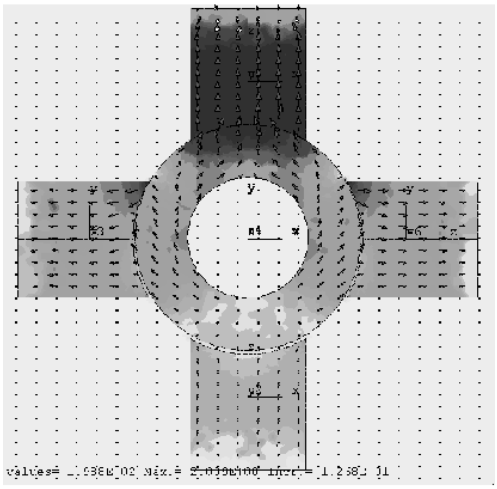

FIGURE 4: Flux density (dark=high density) and direction (arrows) calculated with Flux-3D. This is a cut in the plane C-D depicted in Figure 3

the smallest in the upper pole. As a consequence the flux of the entire permanent magnetic ring tends to pass through the upper pole, leading to a much higher negative stiffness as to be expected from the results achieved with the simplified U-magnet.

Another drawback is a cross-coupling effect between the two radial directions of the control flux Φ_c. Principally a control flux for the *y*-direction should pass through the poles 1 and 3. But certainly the paths 1-2 and 1-4 have the same magnetic resistance, hence the flux generated with coil 1 will partly pass through all poles. As long as the rotor is in the centre position these cross-fluxes result in no force perpendicular to the control current. Assuming the rotor in e. g. the upper right position, the flux created with coil 1 has the smallest magnetic resistance when passing the poles 1 and 2 and is stronger than the opposing flux generated with coil 3. Thereby a force in positive *x*-direction occurs, which depends on the *x*- and *y*-position as well as on the magnitude of the *y*-control current. This results in a third term in the equation for the magnetic force already mentioned by Fukata & Yutani (1996), exemplarily for the *x*-direction:

$$f_x = k_i i_x + k_s x + k_{sxy} \cdot f(x, y, i_y) \qquad (7)$$

HETEROPOLAR DESIGN

To overcome the drawbacks of the homopolar design, the heteropolar arrangement with decoupled directions shown in Figure 5 represents a bearing with optimal behavior with respect to negative stiffness and cross coupling effects. Here three ferromagnetic rings are used to seperate the control fluxes in *x*- and *y*-direction. The center ring holds four permanent magnets to

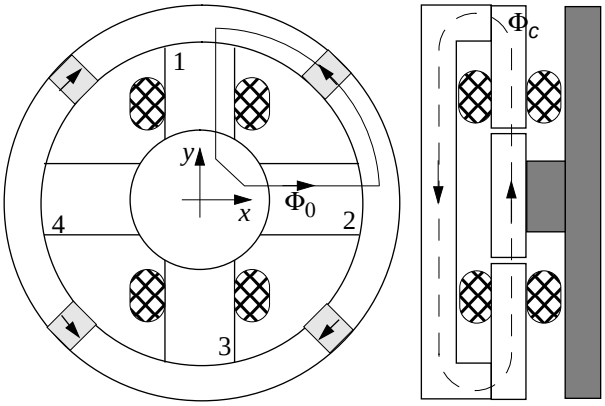

FIGURE 5: Heteropolar Design

create the bias flux in the four connected poles. The left ring is connected with poles 1 and 3, and the right ring (dark grey) with 2 and 4.

To avoid mistakes of 3D calculations due to too strong leakage fluxes in *z*-direction, a slightly modified 2D model depicted in Figure 6 is used for calculations. Here the inner ring holds the permanent magnets, while the outer ring corresponds to one of the control flux rings. The flux lines represent the situation for zero control current and center position of the rotor. An interesting aspect is that roughly 20% of the bias flux passes through the outer ring as leakage flux. To minimize this effect, the space between the rings must be larger which would further increase the required space for this design.

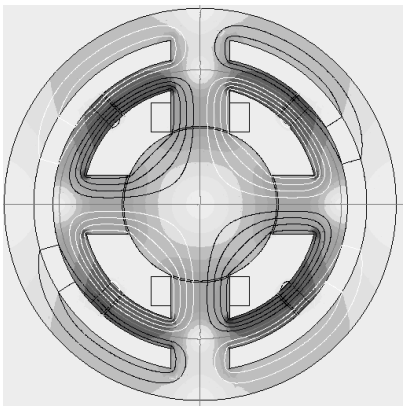

FIGURE 6: Flux-2D model for the heteropolar design. The bias flux density in the airgap is 0.5 T

MEASURED RESULTS

To verify the calculated results a test-rig depicted in Figure 7 has been designed. The shaft with a diameter of roughly 30 mm is connected to a motor with a coupling which has a very high radial and very low axial and

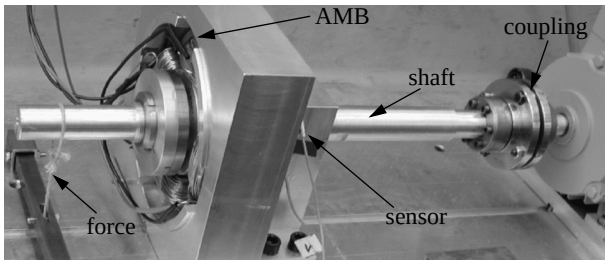

FIGURE 7: Foto of the test-rig

bending stiffness. On the left side the housing and parts of the stator and rotor of the homopolar AMB can be seen and the cables of the eddy current sensors used for position control. On the very left static radial forces can be applied to the rotor.

In Figure 8 the magnetic pressure as a function of the applied control current is shown. To achieve the measured results a slowly in- and decreasing force was applied while the bearing was held in the magnetic centre position with a PID-controller. Beside the globally nonlinear shape, probably caused by iron-saturation, hysteresis effects can be seen. For further calculations a second order polynomial was fit to the data depicted as dashed line. The deviation of measurement and calculation is in a range of approximately 10 %.

To measure the negative stiffness shown in Figure 9, no force was applied and the *x*-position (horizontal) of the rotor was varied within the airgap. The result is the correlation between the control current and the rotor position. Taking (7) and assuming $f_x = f_y = 0$ and thus $k_{sxy} = 0$ the measured polynomial was used to calculate the magnetic pressure from the measured current. A relevant difference between calculation and measurement can be recognised.

To get information about the amount of the cross coupling effect in (7) two calculations were carried out with the 3D model: The solid FE line has been calcu-

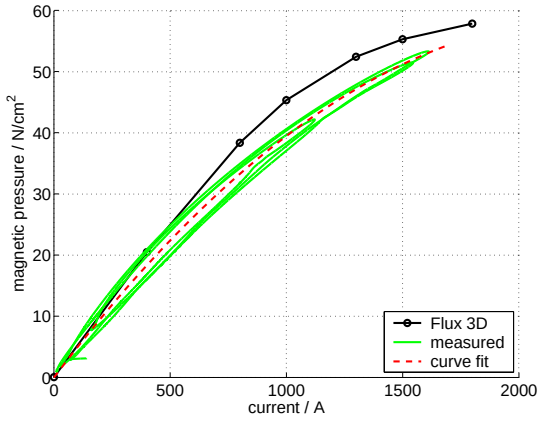

FIGURE 8: 3D calculations and measured results for the homopolar design.

lated without any control current at $y = 0$ and increasing x-position, and the dashed with maximum current i_y in y-direction, while $y = 0$. Both curves differ about 10 %, indicating that cross-coupling exist even in the symmetric case.

To measure the effects of cross coupling several y-positions with different forces in y-direction have been applied while varying the x-position, but in contrast to the FE calculations the slope of all measured curves almost did not vary. Hence for the position control cross coupling effects seem to be negligible.

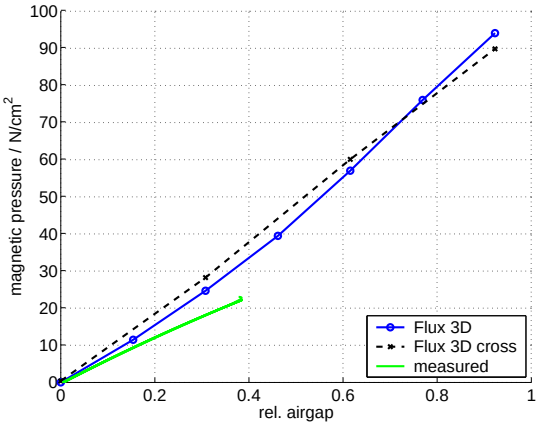

FIGURE 9: Negative stiffness, 3D calculations and measurement

AMB WITH CURRENT BIAS

To compare both PM_0 designs with the I_0-type we briefly describe the used bearing with 8 poles. Hantke (2002) gives a more detailed description.

The outer diameter of the bearing stator is 164 mm, and each pole has a width of 14 mm and a depth of 40 mm. Each polepair has 440 windings, the maximum current is 5 A.

For all bearings the same rotor laminations with an outer diameter of 78.2 mm are used. The nominal airgap s is 0.8 mm for the I_0-type and for all 2D calculations. Unfortunately the airgap for the homopolar design used for the measurements only is 0.65 mm, and the 3D model has the same gap.

COMPARING THE BEARINGS

Finally the calculated results of the three bearings and the 2D and 3D solution of the homopolar bearing shall be compared.

In Figure 10 the magnetic pressure as a function of the control current is shown which corresponds to k_i in (7). In contrast to Figure 2 the 3D solution now is above the 2D solution. There are two likely explanations: first,

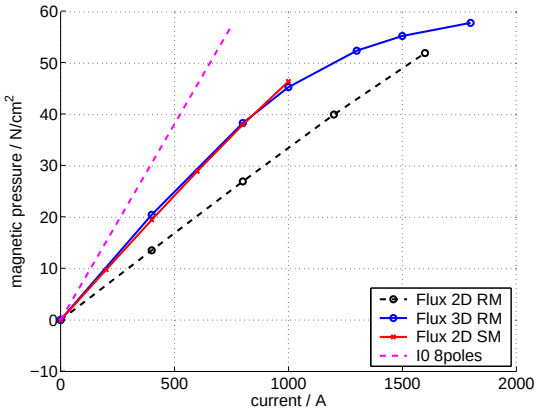

FIGURE 10: Comparison of calculated results. RM and SM indicate the homopolar (**R**otor**M**agnet) and heteropolar (**S**tator**M**agnet) design

the circular permanent magnet on the rotor can be compared with the U-magnet of infinite depth, so there are no stray fluxes “out of the paper plane” in Figure 1. Second, parts of the permanent magnet do not have stator parts in radial direction (see Figure 4), hence for each pole more permanent magnet volume and thus magnetic energy is available.

Comparing the homopolar and heteropolar arrangement, the slope is larger for the second design. The reason is that the control flux only has to pass the airgap twice (SM) instead of four times (RM) so referring to (5) the control flux density should be twice as high. This does not result in a slope 4 times higher because the bias flux was smaller in the heteropolar model.

The I_0-type has the largest slope because the control flux only has to pass the airgap twice, and the described bearing has a very high bias flux density. At $i_0 = 2.5$ A roughly 0.7 T have been measured with a hall probe. The corresponding curve does not saturate because the linearized analytical equation has been used for calculation.

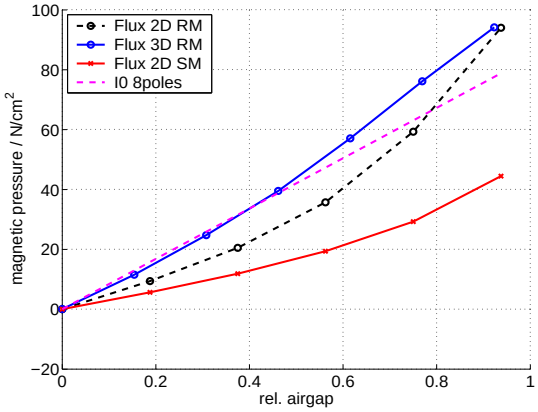

FIGURE 11: Comparing the effect of negative stiffness

In Figure 11 the effects of negative stiffness, corresponding to k_s in (7), are presented. For a better comparison, the relation k_i / k_s will be investigated.

For the I_0-type, where $i_0 = 0.5\ i_{max}$, the maximum control current has to be applied to counteract the negative stiffness force at the maximal airgap for the linear equation, $k_i \cdot i_0 = -k_s \cdot s_0$. Taking the values at 500 A and the relative airgap of 0.4, calculating their ratio and normalizing them such, that the ratio for the I_0-type equals unity, the results shown in the second row of the following table are achieved.

	I_0	2D SM FE	3D RM FE	2D RM meas	2D RM FE
k_i / k_s norm$_{i0}$	1	1.66	0.66	0.77	0.71
L / L_{i0}	1	0.25	0.5		
Vol / Vol_{i0}	1	1.2 - 1.6	0.5		

For the homopolar configuration the changing airgaps for eccentric rotors have a very strong influence on the negative stiffness, and reminding the good results from the simplified considerations, it is obvious that such aspects have to be carefully considered. The ratio will be even worse if the axial airgap between the magnet and both rotor discs is smaller than in the chosen design (see Figure 3). In the worst case this could mean that the control flux is too small to lift the rotor out of the retainer bearings.

The situation is much better for the heteropolar arrangement, but the small negative stiffness is only reached with the space consuming design. The required volume for each design is shown in the last row of the table, assuming that all bearings have roughly the same load capacity, i. e. the same pole surface A and bias flux density B_0.

Finally the inductivity is compared in the third row, again for the same pole surface A and identical maximum currents i_{max}. For the I_0-type B_{max} from (5) is two times higher, because the bias *and* control flux have to be generated by the current. Therefore the inductivity is smaller for the PM_0-types. Moreover the number of airgaps to be passed by the control flux are relevant, so the heteropolar design has the smallest inductivity.

CONCLUSION

The properties of AMBs with and without permanent magnets for the bias flux have been compared. Beside a reduced bearing size, low inductivity and the possibility of zero current control the negative stiffness has to be carefully considered when designing such bearings. Flux paths which are not obvious on the first glance can strongly increase the negative stiffness and thereby deteriorate controllability of the bearing.

As a rule of thumb the heteropolar permanent magnet arrangements seem to be favorable. Since cross coupling effects of the control flux are rather small, probably the heteropolar design presented by Silber & Amrhein (2001) could be a good compromise, where the permanent magnets are arranged radially on extra poles.

Concerning the FE calculations it seems to be difficult to accurately predict the behavior. Especially for finite magnet lengths fluxe leakage appears to be too large in the calculations. In future work the U-magnet and the heteropolar design shall be assembled to measure forces and flux densities and compare them with calculations.

REFERENCES

Blumenstock, K.A., Brown, G.L. (2000): Novel Integrated Radial and Axial Magnetic Bearing, *7th Int. Symp. on Magnetic Bearings*, Zurich, August 2000, pp. 467-471.

Cedrat (2003): CAD Package for electromagnetic and thermal analysis using finite elements.

Fukata, S., Yutani, K. (1996): Characteristics of the Magnetic System of Magnetic Bearing Biased with Permanent Magnets Attached to a Rotor, *5th Int. Symp. on Magnetic Bearings*, Kanazawa, August 96, pp. 395-400

Meins, J. (1997): *Elektromechanik*, Teubner, Stuttgart.

Hantke, A. (2002): *Identifikation und Auswirkung der Rotorverluste verursacht durch ummantelte Magnetlager*, Shaker Verlag, Aachen.

Lee, W.-L., Canders, W.-R., Schumacher, W. (2000): New Approaches for Axial Magnetic Bearings, *7th Int. Symp. on Magnetic Bearings*, Zurich, August 2000, pp. 443-448.

McMullen, P.T., Huynh, C.S., Hayes, R.J (2000): Combination Radial-Axial Magnetic Bearing, *7th Int. Symp. on Magnetic Bearings*, Zurich, August 2000, pp. 473-478.

Mohr, H.-U., Matzschmann, M., Schäffel, C., Michael, S. (2003): Entwurf und Design von Magnetlagern für schnelldrehende Rotoren mit modernen Entwurfsmethoden, *Special Antriebstechnik*, VDI-Konstruktion, pp. 70-72.

Molenaar, A., Van Beek, H. F., Sanders, J.L. (1997): A New Linear Magnetic Bearing Configuration for High Accuracy Positioning, *Proc. of MAG '97, Industrial Conf. and Exhibition on Magnetic Bearings*, Virginia, pp. 313-322

Schweitzer, G., Traxler, A., Bleuer, H. (1993): *Magnetlager*, Springer-Verlag Berlin, Heidelberg, New York.

Silber, S., Amrhein, W. (2001): Magnetic Bearing Sytem, Patent No. WO 01/48389 A2